

J. Environ. Treat. Tech. ISSN: 2309-1185

Journal web link: http://www.jett.dormaj.com



Artificial Neural Network (ANN) Modeling of Cavitation Mechanism by Ultrasonic Irradiation for Cyanobacteria Growth Inhibition

Esmaeel Salami Shahid¹, Marjan Salari ^{2*}, Majid Ehteshami ³, Solmaz Nikbakht Sheibani⁴

¹Ph.D. Candidate of Civil and Environmental Engineering, Shiraz University, Shiraz, Iran ^{2*}Department of Civil Engineering, Sirjan University of Technology, Kerman, Iran ³ Associate Professor, Civil and Environmental Eng. Dept. KN Toosi Univ. of Technology, Tehran, Iran 4 M.Sc. Candidate, Environment Eng. Dept. Shiraz University, Shiraz, Iran

Abstract

Cyanobacteria produce toxins that affect animals and human's health. Therefore, modeling concentration of this type of algae is necessary. This study employs artificial neural network (ANN) modeling method to simulate the cavitation mechanism by ultrasonic irradiation on cyanobacteria concentration variation in treated water. The proposed model used parameters such as power intensity, frequency and the time of ultrasound irradiation as input variables. The results showed that proportional value of cyanobacteria concentration to the initial concentration (C/C_0). The data obtained from a laboratory experiment and number of data in the existed study was not enough for ANN modeling, the data expanded to 7280 data sets from the original 28 data sets obtained by the experimental study. A feed-forward learning algorithm with 20 neurons in the first (hidden) layer and one neuron in the second layer was developed with the MSE value equals to 2.72×10^{-5} . Model results were used for predicting the cell density value. Furthermore, a novel formulation was presented to correlate the C/C_0 values with the cell density. To verify the accuracy of the ANN and developed equation, the value of cell density was predicted by studies performed by other researchers. In this case the MSE was 1.55×10^{-4} .

Keywords: Artificial Neural Networks, Cyanobacteria, Modeling, Ultrasonic irradiation, Water Quality

1 Introduction

Cyanobacteria affect animals and human's health due to poison production. The presence of this type of algae in nutrient-rich drinking water reserves has adverse effects in terms of taste, smell and health (Leclercq et al., 2014). Hence, it is necessary worldwide to control the blooms of algae and to remove the garbage before the distribution of water in an appropriate manner in accordance with the WHO guidelines and customer expectations (Leclercq et al., 2014).

Today, ultrasonic devices have various applications in different fields of science, industry, medical practice and so forth (Sharma et al., 2011). One of the innovative techniques for improvement of water/wastewater treatment process is the application of ultrasonic waves; that does not require the addition of oxidants or catalyst and does not generate additional waste streams as compared to adsorption or ozonation processes (Zhang et al., 2009; Wang and Yuan 2016). The ultrasonic method is known to have a detrimental effect on the structure and function of organisms (Hongwei

et al., 2004). Therefore, ultrasonic irradiation, due to its advantages, including safety, cleanliness and energy conservation, can be a suitable way to reduce pollution in aquatic resources containing harmful algae. Only a few researches have been developed since cyanobacterial bloom control by ultrasound is a fairly new field. Moreover, the ultrasonic process is not affected by the toxicity and low biodegradability of compounds (Fu et al., 2007). Ultrasound waves affect larger molecules faster than smaller ones (Yamamoto et al., 2015). The ultrasonic method uses electrical energy to induce physical, chemical and biological treating effects as shown in Fig.1 (Kasaai, 2013). Sound waves with a frequency between 20 KHz to 200 MHz are called ultrasonic waves. When an ultrasonic wave enters a liquid, it can cause cavitation (Wu et al., 2012). Fig.2 illustrates the ultrasonic range due to its applications. In addition, bloom-forming cyanobacteria participate in diverse consortia, and symbioses with a broad array of microorganisms, higher plants and animals, which help

Corresponding author: Marjan Salari, Department of Civil Engineering, Sirjan University of Technology, Kerman, Iran. E-mail: salari.marjan@gmail.com.

alleviate environmental stresses and limitations (Pilli et al., 2011; Rajasekhar et al., 2012). In this study, the apparent gap between experimental data and modeling, by trying to determine if artificial intelligence models can predict cavitation mechanism for inhibiting algal growth. According to the best author's knowledge, artificial neural network modeling and network performance evaluation are not considered in order to determine the cavitation mechanism by ultrasonic irradiation to control cyanobacterial citrate growth.

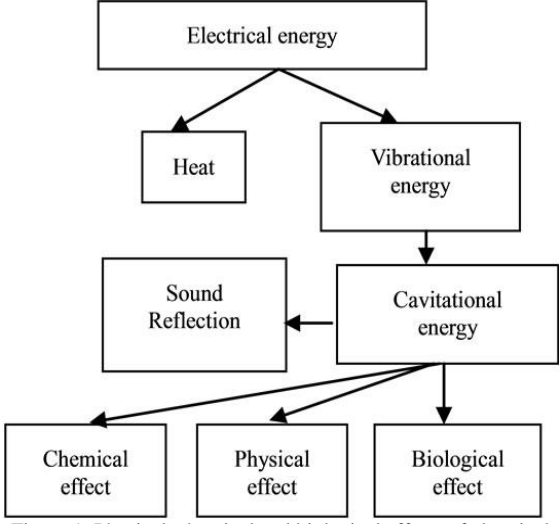


Figure 1: Physical, chemical and biological effects of electrical energy (Kasaai, 2013)

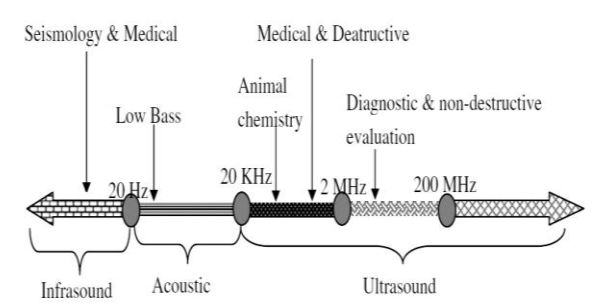


Figure 2: Diagram of the ultrasonic range (Wu et al., 2012)

2 Material and Methods

Three ultrasonic devices, two beaker systems (operating at 200 kHz and 1.7 MHz, respectively) and one horn system (operating at 20 kHz), are employed in this study. The ultrasonic generator designed in our laboratory consists of a voltage-controlled oscillator (VCO) (Zhang et al., 2009), power amplifier, matched impedance and feedback unit. The ultrasound at 20 kHz was emitted from a titanium horn dipped into the cyanobacterial suspension, and the ultrasonic at higher frequencies (200 kHz and 1.7 MHz) was emitted from the piezo-electric discs of lead zirconate titanate fixed on the underside of the beaker reactors with epoxy. Each frequency required a specific emitter. Their ultrasonic powers dissipated in the medium were measured calorimetrically (Paerl, 2018). The volume of ultrasonic

reactors was 1200 and 800 ml cyanobacterial suspension that was filled in experiments (Lee et al., 2002; Ma et al., 2005). Cyanobacteria, or blue-green algae, occur worldwide often in calm, nutrient-rich waters. Some species of cyanobacteria produce toxins that affect animals and humans. People may be exposed to cyanobacteria toxins by drinking or bathing in contaminated water. The most frequent and serious health effects are caused by drinking water containing toxins or by ingestion during recreational water contact like swimming. Cyanobacteria can also cause problems for drinking water treatment systems. Therefore, studying and modeling the concentration of this type of algae is necessary to prevent its adverse effects on humans and animals.

2.1 Cavitation process

When a liquid is sonicated, dissolved gas molecules are entrapped by micro-bubbles that grow and expand upon rarefaction of the acoustic cycle; these micro-bubbles then release extreme temperatures upon adiabatic collapse (Hao et al., 2004; Lin et al., 2008). The process is based on the phenomenon of acoustic cavitation, which involves the formation, growth, and sudden collapse of micro-bubbles that generate short-lived, localized "hot spots" in an irradiated liquid (Wang et al., 2007).

The high-temperatures (5000 K) and pressures (1000 atm) induced by cavitation's in collapsing gas bubbles in aqueous solution lead to the thermal dissociation of water molecules into reactive free radicals H0 and OH0 (Shimizu et al., 2007; Goel et al., 2004). There are three possible reaction sites in ultrasonically irradiated homogeneous liquids: (i) the gaseous interiors of collapsing cavities; (ii) the interfacial liquid region between cavitation's bubbles and the bulk solution, where high-temperatures (ca. 1000-2000 K) and high temperature gradients exist; and (iii) the bulk solution at ambient temperature, where small amounts of OH0 diffuse from the interface. The sonochemical effect takes place at the gas-liquid interface due to the oxidation of organic molecules by OH0 and, to a lesser extent, in the bulk solution or the pyrolytic decomposition inside the bubbles (Li et al., 2008; Eren, 2012). Hydrophilic and non-volatile compounds such as dyes mainly degrade through OH0 mediated reactions in the bulk solution and at the bubbleliquid interface, while hydrophobic and volatile species degrade thermally inside the bubbles (Merouani et al., 2015; Wu et al., 2012).

Cavitation phenomena produce high temperature/pressure fields and free radicals (such as OH^0 and H_2O_2 , etc) in liquids (Fig. 3) (Pang et al., 2011). Cavitation consists of the repetition of three distinct steps: formation (nucleation), rapid growth (expansion) during the cycles until it reaches a critical size, and violent collapse in the liquid in less than a microsecond (Chowdhury and Viraraghavan, 2009) as shown in Fig. 4. Parameters that affect cavitation are liquid temperature, external pressure, liquid viscosity, amount and type of solved gases, the surface tension of a liquid (Fu et al., 2007). All these parameters are related to the liquid but the parameters of sound wave that are effective discuses below:

2.2 Cavitation near surfaces

The most important effects of ultrasonic on liquid-solid

systems are mechanical and attributed to asymmetric cavitation. In addition, shockwaves that have the potential to create microscopic turbulence are produced within interfacial films surrounding nearby solid particles (Pang et al., 2011).

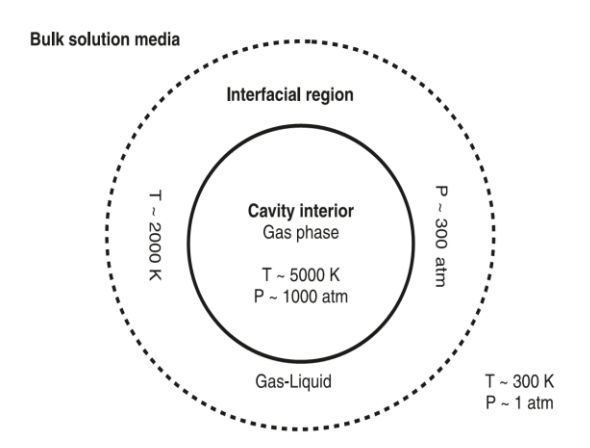


Figure 3: Reaction zone in cavitation process (Aadapted from Duong Pham et al., 2009)

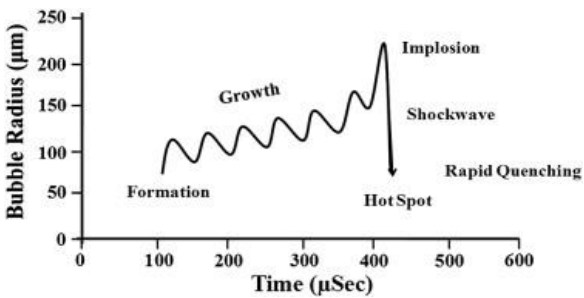


Figure 4: Growth and implosion of cavitation bubbles in aqueous solution under ultrasonic irradiation (Merouani et al., 2015)

Asymmetric collapse leads to the micro-jet formation of solvent that collides with the solid surface at tremendous force, resulting in newly exposed, highly reactive surfaces as well as corrosion and erosion. These phenomena increase the rate of mass transfer near the catalyst surface (Chowdhury and Viraraghavan, 2009).

2.3 Acoustic pressure

The acoustic pressure is a sinusoidal wave dependent on time (t), frequency (f) and the maximum pressure amplitude of the wave, Pa, max and is represented by the following equation (Kuna et al., 2017; Hongwei et al., 2004):

$$P_a = P_{a,\text{max}} \sin(2\pi f.t) \tag{1}$$

where, Pa is the acoustic pressure which directly proportional to more and violent collapse of bubbles, Pa, max is the maximum pressure amplitude of the wave which directly proportional to the input power of the transducer, t and fare time and frequency of ultrasonic waves, respectively (Hongwei et al., 2004; Shchukin et al., 2011). A sufficiently large increase in the intensity of ultrasound will

generate larger values of acoustic pressure. An increase in the value of Pa lead to a more and violent collapse (Hongwei et al., 2004).

Hence frequency has a diverse relation with the bubble sizes, in (relatively) low-frequency irradiations (16-100KHz) will produce large cavitation bubbles which results in high temperature and pressure in the cavitation zone (Tsaih et al., 2004). As the frequency increases the cavitation zone becomes less violent and, in the MHz, range no cavitation's is observed and the main mechanism is acoustic streaming (Hongwei et al., 2004). I, is the power intensity of the ultrasonic wave in terms of the energy transmitted per unit time per unit normal area of fluid:

$$I = P_{a \max}^{2} (2 \rho c)^{-1}$$
 (2)

where ρ is density of a medium/liquid, c is velocity of sound in that medium and P_a is the maximum pressure amplitude of the wave (Hongwei et al., 2004; Shchukin et al., 2011). Increasing intensity will increase the cavitation and also violent collapse of bubbles (Tsaih et al., 2004). This increase will continue until reaching an optimum point and after that point increase in power, the intensity will reduce the rate of cavitation. For example, Mutiarani et al., showed that removing turbidity increases with increasing power to 60 watts and decreases for powers beyond 60w (Zhang et al., 2016). Whereby the effect of power on removal efficiency (of microcystins) was studied using 30, 60 and 90 watt in the constant frequency of 20 KHz after 1, 5, 10, 20 minutes of exposure to the ultrasonic samples. The results are shown in Fig.5.

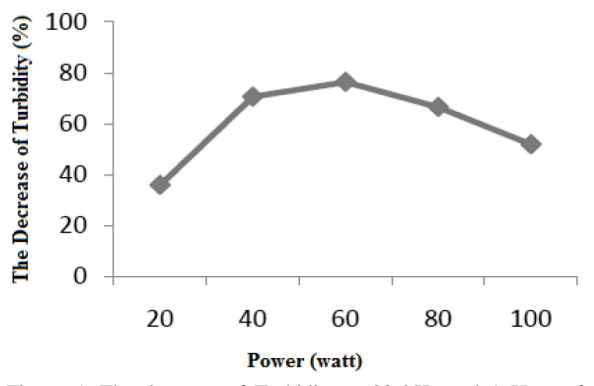


Figure 5: The decrease of Turbidity at 28 kHz and 1 Hour of Irradiation time with variation of Power (Hatanaka et al., 2002)

This phenomenon may be explained by bubble shielding effect. When the power intensity is high enough, a dense cloud of navigational bubbles accumulates around the ultrasonic transducer. The cavitation bubbles attenuate sound waves due to both scattering and absorption and thus impede the propagation of sound waves, especially at the resonant size (Mutiarani and Trisnobudi 2012).

This study intends to develop the ANN model(s) to simulate the concentration of microsystems after using ultrasonic waves to remove them or changing those

pollutants to removable compounds. Input variables such as time, frequency and power of the applied ultrasonic are used to determine the proportional (C/C0) as the target value of the model(s). The data from Ma, et al., are used in this study (Rajasekhar et al., 2012). Then the results are verified by distinct study made by Hao et al., 2004 and Zhang et al., 2016. Ultrasonic wave may Influence Cyanobacteria in several ways: (a) sinking Cyan bacteria by rapture vehicles that filled with gases which causes the flotation of Cyanobacteria; (b) disruption of photosynthesis; (c) damage of cell membranes due to lipid peroxidation; and (d) differential susceptibility to ultrasonic waves at different stages in the cell division cycle (Gerde et al., 2012; Zhang et al., 2006). Most experiments in this field are performed in frequencies between 20-28 KHz and in some researchers used frequencies up to 1.7 MHz (Lee et al., 2002; Ma et al., 2005). Therefore, this study evaluates the effect of different ultrasonic frequencies such as 20,150,410 and 1700 KHz (in constant power of 30w) after 1,5,10 and 20 minutes of irradiation on Microcystis as the typical representative of bloom-forming algae.

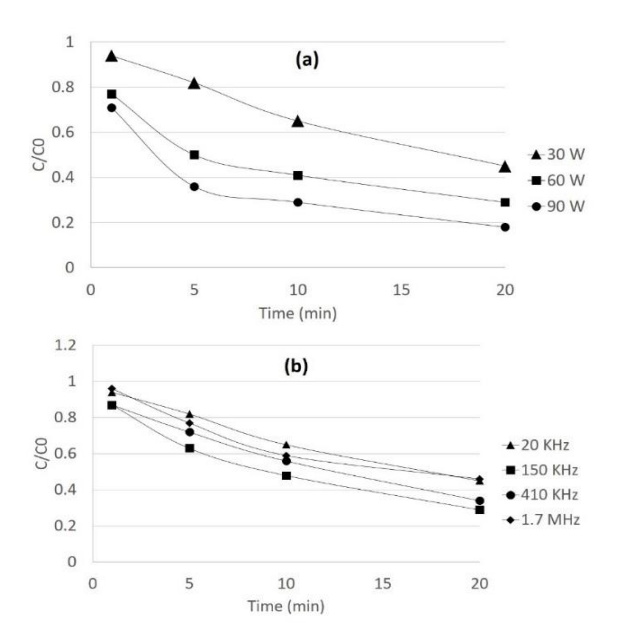


Figure 6: (a) The removal of microcystins dissolved in water after ultrasonic irradiation at 20 kHz and various powers of 30, 60, and 90 W with time (Hatanaka et al., 2002) and (b) The removal of microcystins dissolved in water after ultrasonic irradiation at 30W and various frequencies of 20, 150, 410 kHz, and 1.7 MHz with time (Hao et al., 2004)

Also, some research worked on the effect of ultrasonic irradiation on cyanobacteria. Their work is very similar to (Ma et al., 2005). In both works (see Fig.6) they used UV–vis spectrophotometer (Ultra-Spec 2000, Amersham Biosciences AB, Uppsala, Sweden). Furthermore, Ma et al., calibrated the device on 684 nm and Hao et al., found an optical density of cell suspension of 560 nm as an optimum. The initial concentration in both experiments was $2\mu g/L$. Therefore, it is possible to compare the results of the current ANN model with (Ma et al., 2005; Hao et al., 2004).

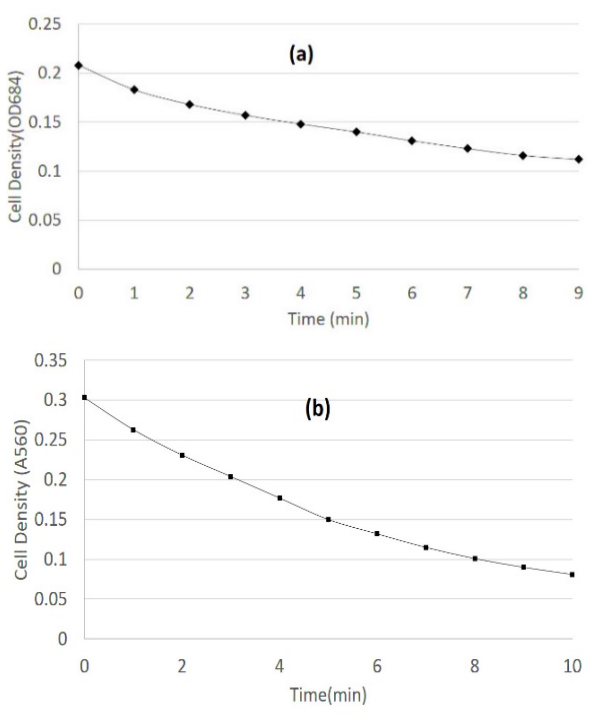


Figure 7: (a) Effect of ultrasonic irradiation (20 kHz, 30 W) for different time on Microcystis suspension, including changes of Microcystis biomass (Lee et al., 2002) and (b) Cyanobacterial biomass as a function of time during ultrasonic irradiation at 20 kHz, 40W (Ma et al., 2005)

2.4 Artificial Neural Network Method

The artificial neural network (ANN), as its name implies, is a technique for simulation of the human brain functions during the problem-solving process, which has been developed and originated about 60 years ago. The neural network approach can be applied to the powerful computation of complex nonlinear relationships, just as humans apply knowledge gained from past experience to new problems or situations (Tang et al., 2004). Thus, for modeling parameters that don't have a simple (linear) relationship with input data, ANN method can be employed effectively. The MLF (multilayer feed-forward) networks trained with back-propagation algorithm are the most popular type of networks (Salami et al., 2016 a,b; Salari et al., 2018). For example, models that marked by (*) in Table 2 have used feed-forward networks for their development (Tang et al., 2004).

2.5 Structure of the Networks

The basic architecture consists of three types of neuron layers: input, hidden, and output layers. Fig. 10 shows a two-layer network. In feed-forward ANN networks, the signal flow from input to output units, strictly in a feed-forward direction (Samani et al., 2007; Koncsos, 2010). Hidden layers consist of a different number of neurons. Fig. 8 shows a parameter such as "a" is the output of neuron and "p" is the input. Parameters w and p are weight and bias respectively. All parameters denoted as matrices, and can be expressed as (Salami et al., 2015).

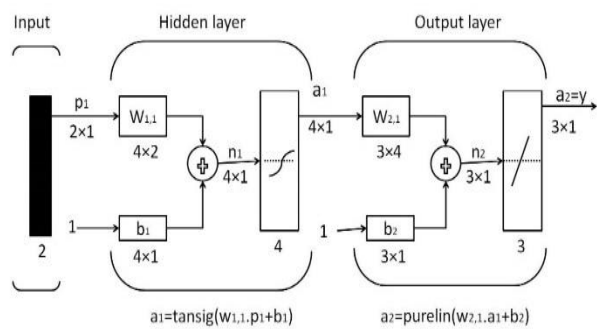


Figure 8: A two layer feed-forward network

$$a = f(net) = f(n) = f(w^{T}.p + b) = f(\sum_{i=1}^{R} w_{R}^{T}.p_{R} + b)$$
 (3)

$$p = [p_1, p_2, ..., p_R], w = [w_1, w_2, ..., w_R]$$
(4)

The most common "f" functions are presented in Fig. 9. These transfer functions transfer output of each layer to a simpler more useful expression for calibrating the wi and bi (s) in next layer/step.

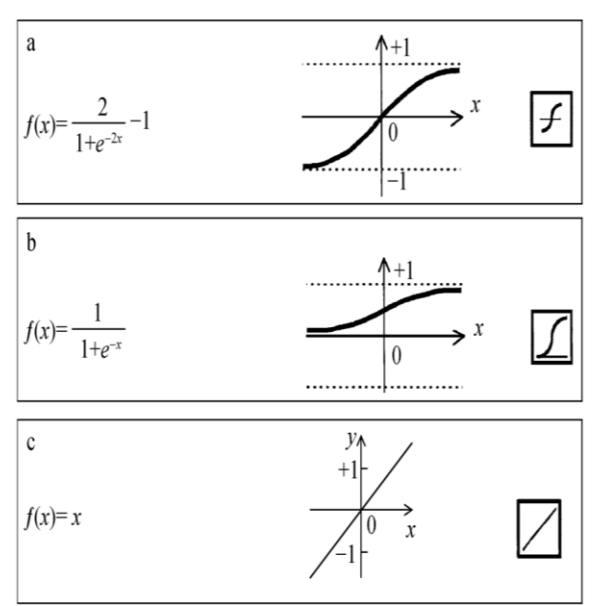


Figure 9: Transfer functions

The training process determines the ANN weights and is similar to the calibration of a mathematical model. In order to perform training correctly, we must iteratively continue and repeat the process of calibrating and optimizing the wi, bi(s), with the final target of minimizing the mean square error (MSE) value as possible as it is, the process will continue until the required precisions reached. In the following procedure, weights and biases will change every time the process is repeated. The calibration process for wi, bi(s) is as (Abraham et al., 2005):

$$W_{i,j}^{(l+1)} = W_{i,j}^{(l)} - \alpha \frac{\partial e(w,b)}{\partial W_{i,j}^{(l)}}$$
(5)

$$b_{i,j}^{(l+1)} = b_{i,j}^{(l)} - \alpha \frac{\partial e(w,b)}{\partial b_{i,j}^{(l)}}$$
(6)

$$\frac{\partial e(w,b)}{\partial \boldsymbol{W}_{i,j}^{(l)}} = \left[\frac{1}{m} \sum_{i=1}^{m} \frac{\partial}{\partial \boldsymbol{W}_{i,j}^{(l)}} e(w,b;\boldsymbol{\chi}^{(l)},\boldsymbol{y}^{(l)}) \right] + \alpha \boldsymbol{W}_{i,j}^{(l)}$$
(7)

$$\frac{\partial e(w,b)}{\partial \boldsymbol{b}_{i,j}^{(l)}} = \left[\frac{1}{m} \sum_{i=1}^{m} \frac{\partial}{\partial \boldsymbol{b}_{i,j}^{(l)}} e(w,b;\boldsymbol{\chi}^{(i)},\boldsymbol{y}^{(i)})\right] + \alpha \boldsymbol{b}_{i,j}^{(l)}$$
(8)

$$mse = \frac{1}{m} \sum_{i=1}^{n} e^2 = \frac{1}{m} \sum_{i=1}^{n} (t_i - a_i)^2$$
 (9)

where α is the learning rate. In this study, the mean square error (MSE) is the criterion for comparing the outputs. Where ti is the target (real) value and ai is the network output. Two feed-forward networks with back propagation learning rule (Eqs.9-12) are used to develop the models in MATLAB environment. The design parameters of the networks have been. Other training parameters of the models are shown in Table 1.

Table 1: Training parameters

αο	0.001	Network type	Feed-Forward back propagation
α decrees	0.1	Training function	Trainlm (Levenberg- Marquardt)
α increase	10	Adaptive learning function	Train GDM
maximum α	1E+10	Performance function	MSE
min grad	1.00E-10	Transfer function	Tensing(x)

validation of all equations/models after development, have been tested with precision parameters such as R or R* and MAE. R* is used in cases that we had negative values of R. In other words, when $y_i > \overline{y_i}$, R will be negative.

$$R = \frac{\sum_{j=1}^{i} 1 - \frac{\left|\overline{y}_{j} - y_{j}\right|}{\overline{y}_{j}}}{i}$$

$$\begin{cases} for \ y_{j} > \overline{y}_{j} \to R_{1} = \sum \frac{\overline{y}_{j}}{\overline{y}_{j}} \\ for \ y_{j} < \overline{y}_{j} \to R_{2} = \sum \frac{\overline{y}_{j}}{\overline{y}_{j}} \end{cases}$$

$$R^{*} = \frac{R_{1} + R_{2}}{i}$$

$$MAI = \frac{\sum_{j=1}^{i} \left|y_{j}^{-} - y_{j}\right|}{i}$$

$$(11)$$

(11)

3 Results and Discussion

3.1 Data development

Fig.6 shows measured data that can be used in this study. They are just 28 sets (12 sets obtained from Fig.6a and 16 sets obtained from Fig.6b). Since the size of data sets did not look enough for developing a reliable ANN model, we used a simple interpolation method to expand these 28 sets of data to 7280 sets (Hao et al., 2004). To implement the procedure all three (input) parameters of time (t), power (I) and frequency (f) were prepared with smaller intervals compared to Fig 6 (a,b). Actually, the number of data was increased to a reasonably sufficient amount by simple interpolation. For example, in step 1, the irradiation duration was modified from 1 to 20 min, one minute by minute. In step 2, power changed from 30W to 90W by 10W each time, and in step 3 the frequency range expanded from 20 to 400 KHz by 10 KHz and from 500 KHz to 1.7 MHz by 100 KHz each time. Furthermore, all possible compositions of input parameters were considered in the potential range.

In order to ensure the model accuracy, the original data (28 data sets from Ma et al., (2005) removed from learning data and just were used to validate the models after the development. Since $Ln(C/C_0)$ exhibited a rather linear relationship with time, it was chosen as the target value to obtain a more accurate and reliable model. The target values of 7280 data sets prepared and adjusted for modelling are presented in Fig. 10.

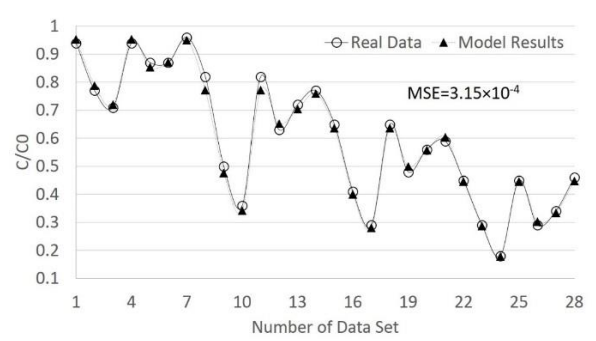


Figure 11: Comparison between model results and real data

3.2 Cell density simulation

Input parameters such as Fig. 6a data, (I = 30 W, f = 20 KHz, t = 0, 1, 2..., 9 min) were used as input parameters in the ANN model and C/C_{θ} for all 10 conditions were simulated. Then a novel formula such as Eq. (13-15) is developed to show the relationship between the C/C_{θ} and cell density.

$$cell density = \frac{x_m}{a_0 + \frac{t.(a_e - a_0)}{T}}$$
 (13)

$$a_0 = \frac{x_{m,0}}{x_0} \tag{14}$$

$$a_e = \frac{x_{m,e}}{x_m} \tag{15}$$

where $x_{m,0}$ is the C/C_0 in t=0, calculated with Eq. 11, x_0 is cell density in t=0, obtained from Fig. 6a, $x_{m,e}$ is C/C_0 in end time (T), calculated with Eq. 11, x_e is cell density in end time (T), obtained from Fig. 6a. Fig. 12 shows the results of the model and developed equation (Eq. 13) and their comparison with the real data (Fig. 6a). The input parameters in Fig. 6.b such as (I = 40W, f = 30 KHz, t = 0, 1, 2, ..., 10 min) were used in the generated model and the results of model (r) is converted to cell density using Eq. 13. Finally, the results of the proposed procedure is compared with the results of Hao et al., (2004) which is shown at Fig. 12b.

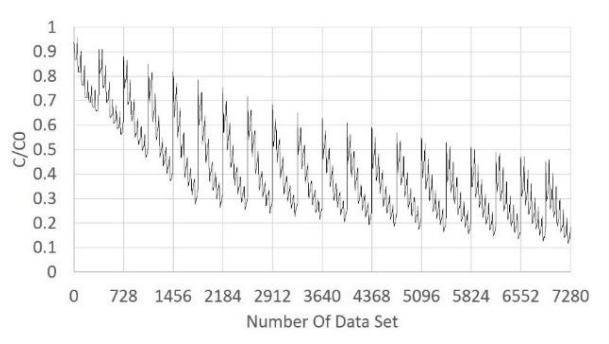


Figure 10: 7280 obtained target values of 7280 data sets prepared for modeling

In order to obtain the optimum removal rate at each condition, we consider all possible combinations of input values (time (t), power (I), frequency (f)) within the desired ranges which can describe the oscillating pattern of the target data C/C_0 . The primary proposed models developed and verified assuming linear or polynomial correlations between input values time (t), power (I) and frequency (f) to the target parameter $Ln(C/C_0)$. However, the analysis showed a weak correlation for linear and polynomial models. Therefore, MATLAB software was used to generate ANN models by applying the input parameters such as I,t and f as feed data to predict $Ln(C/C_0)$ as the target element.

In this regard, 7280 sets of data were used for modelling in which 70% for training, 15% for validation and the other 15% for testing. The network that is used has one hidden layer with 20 neurons. After developing the model, all 7280 (sets of) input data were used to estimate $Ln(C/C_0)$ for each data set, the overall average MSE was $2.72 \times 10-5$ which implies how accurate the model is. Figure 11 shows all 28 sets of original data that were used for modelling compared with model results. The average MSE for the following 28 data sets was $3.15 \times 10-4$. Accordingly, the model outcome is Ln of C/C_0 .

$$x_m = \frac{c}{c_0} = e^r \tag{12}$$

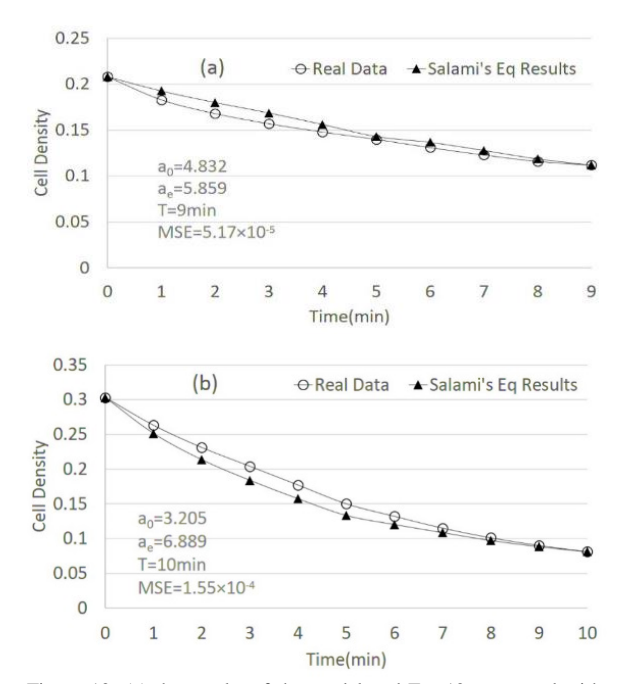


Figure 12: (a) the results of the model and Eq. 12 compared with real data and (b) Model verification using the comparative results of (Hao et al., 2004)

Whereby, the input parameters in Fig.6.b (I = 40W, f = 30 KHz, t = 0, 1, 2, ..., 10 min) were entered to model and the results (r) converted to cell density using Eq. 12 which can be compared to the results of (Hao et al., 2004). It worth to note that the model predicts the value of C/C_0 closely near to 1 in time zero while the data less than one minute were not used at the model training stage. The model results can be used for:

- Optimizing problems
- Calibrating measurement equipment
- Finding errors in measurements, caused by operator/equipment fault
- Reproducing missing/bad data

The other main outcome of the current study is the relation between C/C0-removal and cell density which leads to develop a promising state-of-the-art equation called Salami's equation:

SalamiEq =
$$\alpha \cdot \frac{C}{C0} = \frac{C/C0}{a_0 + \frac{t.(a_e - a_0)}{T}}$$
 (16)

where α is a factor that depends on the passed time, initial and endpoint values of the (C/C_{θ}) and it's proportional to the value of cell density. The value of the (C/C_{θ}) can be obtained from the experiment and/or the presented ANN model. The model simulates C/C_{θ} very close to 1 at time t equals to zero. It is obvious that C in time zero should be equals to C_{θ} and thus the C/C_{θ} must be 1. However, it should be considered that the model is just using times equals or above one minute and the fact that it can predict the behavior of target in time zero, indicate that the model has some kind of intelligence for predicting data that has never encountered before.

4 Conclusion

In recent times wastewater treatment by ultrasonic has become a popular treatment technique due to its ability to degrade pollutants at the end of treating products, i.e. CO₂, water and organic acids. Ultrasonic dye degradation is a complete, irreversible degradation process that provides an appropriate, safe wastewater treatment method with nontoxic and stable products. The main achievement of this study is an ANN model that can simulate the value of $Ln(C/C_0)$, for cyanobacteria at minutes of ultrasound irradiation such as t; with frequency of 'f' and power intensity of 'I'. By using parameters such as I, f and t (as input parameters), model will simulate the value of $Ln(C/C_0)$. Accuracy of the model demonstrated in all domains as Time: between 0 to 20 minutes, Power intensity: between 30 to 90 watts, Frequency between 20 KHz to 1.7 MHz, Initial concentration of cyanobacteria: 2 µg/L. The model has the ability of adaptation with new data and can be updated/calibrated with new/different data. Result of the ANN model and Salami's equation (that both made by data from Ma et al., 2005, verified completely with an outstanding, but similar work such as Hao et al., 2004. This study also shows a method for expanding data with a simple interpolation technique that can increase the number of data (sets) by:

- Breaking the differences between (existed) input parameters to smaller fractions and find values of target parameters (in those points) by interpolation
- Combining different experiment that is done in similar conditions
- Considering all possible combinations of input parameters; and it is a procedure that can be used to describe experimental data sets.

Acknowledgments

The authors are grateful and thankful of Civil and Environmental Laboratory at Shiraz University for providing facilities and apparatus for the current study and analyses.

Ethical issue

Authors are aware of, and comply with, best practice in publication ethics specifically with regard to authorship (avoidance of guest authorship), dual submission, manipulation of figures, competing interests and compliance with policies on research ethics. Authors adhere to publication requirements that submitted work is original and has not been published elsewhere in any language.

Competing interests

The authors declare that there is no conflict of interest that would prejudice the impartiality of this scientific work.

Authors' contribution

All authors of this study have a complete contribution for data collection, data analyses and manuscript writing.

References

- Abbasi M, Asl NR. Sonochemical degradation of Basic Blue 41 dye assisted by nanoTiO2 and H2O2. Journal of hazardous materials. 2008 May 30;153(3):942-7.
- Abraham A. Artificial neural networks. Handbook of measuring system design. 2005 Jul 15.
- 3 Barzamini R, Menhaj MB, Kamalvand S, Tajbakhsh A. Short term load forecasting of Iran national power system using artificial neural network generation two. In2005 IEEE Russia Power Tech 2005 Jun 27 (pp. 1-5). IEEE.
- 4 Chowdhury P, Viraraghavan T. Sonochemical degradation of chlorinated organic compounds, phenolic compounds and organic dyes—a review. Science of the total environment. 2009 Apr 1;407(8):2474-92.
- 5 Pham TD, Shrestha RA, Virkutyte J, Sillanpää M. Recent studies in environmental applications of ultrasound. Canadian Journal of Civil Engineering. 2009 Nov;36(11):1849-58.
- 6 Eren Z. Ultrasound as a basic and auxiliary process for dye remediation: a review. Journal of Environmental Management. 2012 Aug 15;104:127-41.
- 7 Fu H, Suri RP, Chimchirian RF, Helmig E, Constable R. Ultrasound-induced destruction of low levels of estrogen hormones in aqueous solutions. Environmental science & technology. 2007 Aug 15;41(16):5869-74.
- 8 Goel M, Hongqiang H, Mujumdar AS, Ray MB. Sonochemical decomposition of volatile and non-volatile organic compounds—a comparative study. Water Research. 2004 Nov 1;38(19):4247-61.
- 9 Gerde JA, Montalbo-Lomboy M, Yao L, Grewell D, Wang T. Evaluation of microalgae cell disruption by ultrasonic treatment. Bioresource technology. 2012 Dec 1;125:175-81.
- 10 Hao H, Wu M, Chen Y, Tang J, Wu Q. Cavitation mechanism in cyanobacterial growth inhibition by ultrasonic irradiation. Colloids and Surfaces B: Biointerfaces. 2004 Feb 15;33(3-4):151-6.
- 11 Hatanaka SI, Yasui K, Kozuka T, Tuziuti T, Mitome H. Influence of bubble clustering on multibubble sonoluminescence. Ultrasonics. 2002 May 1;40(1-8):655-60.
- 12 Hao H, Wu M, Chen Y, Tang J, Wu Q. Cavitation mechanism in cyanobacterial growth inhibition by ultrasonic irradiation. Colloids and Surfaces B: Biointerfaces. 2004 Feb 15;33(3-4):151-6.
- 13 Kasaai MR. Input power-mechanism relationship for ultrasonic irradiation: Food and polymer applications.
- 14 Koncsos T., The application of neural networks for solving complex optimization problems in modeling. In Conference of Junior Researchers in Civil Engineering, 2010. pp. 97-102.
- 15 Kuna E, Behling R, Valange S, Chatel G, Colmenares JC. Sonocatalysis: a potential sustainable pathway for the valorization of lignocellulosic biomass and derivatives. InChemistry and Chemical Technologies in Waste Valorization 2017 (pp. 1-20). Springer, Cham.
- 16 Lee TJ, Nakano K, Matsumura M. A novel strategy for cyanobacterial bloom control by ultrasonic irradiation. Water Science and Technology. 2002 Sep;46(6-7):207-15.
- 17 Li M, Li JT, Sun HW. Decolorizing of azo dye Reactive red 24 aqueous solution using exfoliated graphite and H2O2 under ultrasound irradiation. Ultrasonics Sonochemistry. 2008 Jul 1;15(5):717-23.
- 18 Leclercq DJ, Howard CQ, Hobson P, Dickson S, Zander AC, Burch M. Controlling cyanobacteria with ultrasound. InINTER-NOISE and NOISE-CON Congress and Conference Proceedings 2014 Oct 14 (Vol. 249, No. 3, pp. 4457-4466). Institute of Noise Control Engineering.
- 19 Lin JJ, Zhao XS, Liu D, Yu ZG, Zhang Y, Xu H. The decoloration and mineralization of azo dye CI Acid Red 14 by sonochemical process: rate improvement via Fenton's reactions. Journal of Hazardous Materials. 2008 Sep 15;157(2-3):541-6.

- 20 Merouani S, Ferkous H, Hamdaoui O, Rezgui Y, Guemini M. A method for predicting the number of active bubbles in sonochemical reactors. Ultrasonics sonochemistry. 2015 Jan 1:22:51-8.
- 21 Muthukumaran S, Kentish SE, Stevens GW, Ashokkumar M. Application of ultrasound in membrane separation processes: a review. Reviews in chemical engineering. 2006;22(3):155-94.
- 22 Mutiarani IM., and Trisnobudi A. Ultrasonic Irradiation in Decreasing Water Turbidity, 2009..
- 23 Ma B, Chen Y, Hao H, Wu M, Wang B, Lv H, Zhang G. Influence of ultrasonic field on microcystins produced by bloom-forming algae. Colloids and Surfaces B: Biointerfaces. 2005 Mar 25;41(2-3):197-201.
- 24 Pilli S, Bhunia P, Yan S, LeBlanc RJ, Tyagi RD, Surampalli RY. Ultrasonic pretreatment of sludge: a review. Ultrasonics sonochemistry. 2011 Jan 1;18(1):1-8.
- 25 Pang YL, Abdullah AZ, Bhatia S. Review on sonochemical methods in the presence of catalysts and chemical additives for treatment of organic pollutants in wastewater. Desalination. 2011 Aug 15;277(1-3):1-4.
- 26 Paerl HW. Mitigating toxic planktonic cyanobacterial blooms in aquatic ecosystems facing increasing anthropogenic and climatic pressures. Toxins. 2018 Feb;10(2):76.
- 27 Rajasekhar P, Fan L, Nguyen T, Roddick FA. A review of the use of sonication to control cyanobacterial blooms. Water research. 2012 Sep 15;46(14):4319-29.
- 28 Shimizu N, Ogino C, Dadjour MF, Murata T. Sonocatalytic degradation of methylene blue with TiO2 pellets in water. Ultrasonics sonochemistry. 2007 Feb 1;14(2):184-90.
- 29 Shchukin DG, Skorb E, Belova V, Moehwald H. Ultrasonic cavitation at solid surfaces. Advanced Materials. 2011 May 3:23(17):1922-34.
- 30 Salami ES, Salari M, Ehteshami M, Bidokhti NT, Ghadimi H. Application of artificial neural networks and mathematical modeling for the prediction of water quality variables (case study: southwest of Iran). Desalination and Water Treatment. 2016 Dec 1;57(56):27073-84.
- 31 Salari M, Shahid ES, Afzali SH, Ehteshami M, Conti GO, Derakhshan Z, Sheibani SN. Quality assessment and artificial neural networks modeling for characterization of chemical and physical parameters of potable water. Food and Chemical Toxicology. 2018 Aug 1;118:212-9.
- 32 Norman ES, Dunn G, Bakker K, Allen DM, De Albuquerque RC. Water security assessment: integrating governance and freshwater indicators. Water Resources Management. 2013 Jan 1;27(2):535-51.
- 33 Samani N, Gohari-Moghadam M, Safavi AA. A simple neural network model for the determination of aquifer parameters. Journal of Hydrology. 2007 Jun 30;340(1-2):1-1.
- 34 Salami ES, Ehteshami M. Simulation, evaluation and prediction modeling of river water quality properties (case study: Ireland Rivers). International journal of environmental science and technology. 2015 Oct 1;12(10):3235-42.
- 35 Chen D, Sharma SK, Mudhoo A. Handbook on applications of ultrasound: sonochemistry for sustainability. CRC press; 2011 Jul 26
- 36 Tsaih ML, Tseng LZ, Chen RH. Effects of removing small fragments with ultrafiltration treatment and ultrasonic conditions on the degradation kinetics of chitosan. Polymer degradation and stability. 2004 Oct 1;86(1):25-32.
- 37 Tang JW, Wu QY, Hao HW, Chen Y, Wu M. Effect of 1.7 MHz ultrasound on a gas-vacuolate cyanobacterium and a gasvacuole negative cyanobacterium. Colloids and Surfaces B: Biointerfaces. 2004 Jul 15;36(2):115-21.
- 38 Wang J, Jiang Y, Zhang Z, Zhang X, Ma T, Zhang G, Zhao G, Zhang P, Li Y. Investigation on the sonocatalytic degradation of acid red B in the presence of nanometer TiO2 catalysts and

- comparison of catalytic activities of anatase and rutile TiO2 powders. Ultrasonics sonochemistry. 2007 Jul 1;14(5):545-51.
- Wu TY, Guo N, Teh CY, Hay JX. Advances in ultrasound technology for environmental remediation. Springer Science & Business Media; 2012 Oct 20.
- 40 Wang M, Yuan W. Modeling bubble dynamics and radical kinetics in ultrasound induced microalgal cell disruption. Ultrasonics sonochemistry. 2016 Jan 1;28:7-14.
- 41 Wu X, Joyce EM, Mason TJ. Evaluation of the mechanisms of the effect of ultrasound on Microcystis aeruginosa at different ultrasonic frequencies. Water research. 2012 Jun 1;46(9):2851-8.
- 42 Yamamoto K, King PM, Wu X, Mason TJ, Joyce EM. Effect of ultrasonic frequency and power on the disruption of algal cells. Ultrasonics sonochemistry. 2015 May 1;24:165-71.
- 43 Zhang H, Zhang J, Zhang C, Liu F, Zhang D. Degradation of CI Acid Orange 7 by the advanced Fenton process in combination with ultrasonic irradiation. Ultrasonics sonochemistry. 2009 Mar 1;16(3):325-30.
- 44 Zhang G, Zhang P, Liu H, Wang B. Ultrasonic damages on cyanobacterial photosynthesis. Ultrasonics Sonochemistry. 2006 Sep 1;13(6):501-5.
- 45 Wang M, Yuan W. Modeling bubble dynamics and radical kinetics in ultrasound induced microalgal cell disruption. Ultrasonics sonochemistry. 2016 Jan 1;28:7-14.